KERNFORSCHUNGSZENTRUM

KARLSRUHE

Oktober 1967

KFK 628
SM 101/12
EUR 3672 e

Institut für Neutronenphysik und Reaktortechnik

# The Group Cross-Section Set KFK-SNEAK. Preparation and Results

H. Bachmann, H. Huschke, E. Kiefhaber, B. Krieg, H. Küsters,
M. Metzenroth, I. Siep, K. Wagner, D. Woll



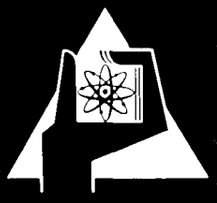

Gesellschaft für Kernforschung m.b.H.
Karlsruhe

# Erratum

zum Bericht: KFK 628; SM 101/12; EUR 3672 e / Oktober 1967

THE GROUP CROSS-SECTION SET KFK-SNEAK. PREPARATION AND RESULTS

von
H. Bachmann, H. Huschke, E. Kiefhaber, B. Krieg, H. Küsters
M. Metzenroth, I. Siep, K. Wagner, D. Woll

In Table III a factor of $10^{-1}$ is missing for $\sigma_c$(U238) / $\sigma_f$(U235).

On page 7 replace N(Cr) = $1.27 \cdot 10^{-2}$ by N(Cr) = $3.42 \cdot 10^{-3}$,

add N(Fe) = $1.27 \cdot 10^{-2}$

KERNFORSCHUNGSZENTRUM KARLSRUHE

Oktober 1967

KFK 628
SM 101/12
EUR 3672 e

Institut für Neutronenphysik und Reaktortechnik

# The Group Cross-Section Set KFK-SNEAK. Preparation and Results[+)]

H. Bachmann, H. Huschke, E. Kiefhaber, B. Krieg, H. Küsters
M. Metzenroth, I. Siep, K. Wagner, D. Woll

Gesellschaft für Kernforschung m.b.H., Karlsruhe

[+)] Work performed within the association in the field of fast reactors between the European Atomic Energy Community and Gesellschaft für Kernforschung m.b.H., Karlsruhe.

INTERNATIONAL ATOMIC ENERGY AGENCY

SYMPOSIUM ON FAST REACTOR PHYSICS AND RELATED SAFETY PROBLEMS

30 October - 3 November

Kernforschungszentrum Karlsruhe, Germany

---

SM 101/12

# THE GROUP CROSS-SECTION SET KFK-SNEAK. PREPARATION AND RESULTS[+]

H. Bachmann, H. Huschke, E. Kiefhaber, B. Krieg, H. Küsters
M. Metzenroth, I. Siep, K. Wagner, D. Woll

## 1. INTRODUCTION

The lack of accuracy in some essential cross section types gives rise to considerable fluctuations in some important quantities used in the design of large fast reactors. As far as only concepts are regarded and trends of main integral nuclear parameters are of interest, the theoretical methods and basic data used today are able to give satisfactory answers. But in calculating the nuclear properties of a fast reactor, really built or to be built, with the feedback on thermodynamic and economic properties, safety and long-time characteristics one obtains remarkable differences with different basic data recommended by various authors. Looking at integral reactor quantities shown in the intercomparisons at the Argonne Conferences in 1965 and 1966 the accuracy in the calculation of fast reactors is improving with time, but convergence of the results has not yet been reached.

In Karlsruhe the fast critical assembly SNEAK is operating since December 1966. The theoretical analysis of the experiments clearly should be done on the basis of the latest and best cross-section data and method. Up to 1965 we calculated fast reactors with the Russian group constant set ABN from Bondarenko et.al. [1].

---

[+] Work performed within the association in the field of fast reactors between the European Atomic Energy Community and Gesellschaft für Kernforschung mbH., Karlsruhe.

In 1965 J.J. Schmidt revised his first cross-section evaluation [2], and on this basis we prepared new infinite dilute group constants, with a weighting spectrum of a typical 1000 MW(e) sodium cooled reactor, for the most important materials used in fast breeders. The resonance self-shielding factors were taken from the Russian set with only slight modifications in the shielding of elastic moderation in certain groups. Preparation of this group constant set KFK 26-10 and results for large power reactors and critical assemblies are given in ref. 3.

In 1966 a second revision of microscopic data has been published by J.J. Schmidt [4]. The recommended cross sections and statistical parameters are available on the Karlsruhe Nuclear Data File KEDAK. From these data we prepared the group cross section set KFK-SNEAK in 26 groups with resonance self-shielding factors calculated by ourselves. It should be noted that no adjustment to the special assembly has been made. The term "SNEAK" in the group set arises from the fact that as a weighting spectrum for averaging the cross-sections a smoothed 26 group collision density spectrum has been used which was calculated with KFK 26-10 for the assembly SNEAK 3A-2. The hydrogen density used in this core is also typical for a large steam cooled fast reactor ($0.07\ g/cm^3$). This is twice the hydrogen density of the assembly SNEAK-1, which has been analysed experimentally during the last months [5].

This paper will give a short survey of the methods used in calculating the group constants. A comparison of the main differences in the basic data is shown. During the preparation of the group constant set the influence of the new data on interesting integral quantities for SNEAK 3A-2 is studied. For the assembly SNEAK 3A-1 under experimental investigation now the essential results and a first conclusion about the quality of the set is given. In a further chapter some results of calculations with the SNEAK-set for ZPRIII/48 and for large sodium and steam cooled reactors will be discussed.

## 2. MICROSCOPIC GROUP CONSTANTS

### 2.1. Theoretical Aspects

The main calculational techniques are described in this chapter. Besides the determination of the elastic removal group constants the effective microscopic group cross section of type z in group g for isotope k is calculated by

$$(1) \qquad {}^{k}\sigma^{g}_{z} = \frac{\int_{(g)} \frac{{}^{k}\sigma_{z}(E)}{{}^{k}\sigma_{t}(E)+\sigma^{g}_{o}} F(E)dE}{\int_{(g)} \frac{F(E)}{{}^{k}\sigma_{t}(E)+\sigma^{g}_{o}} dE}$$

The collision density F(E) is a slowly varying function with respect to energy and composition. In the broad structural resonances F(E) is proportional to the effective logarithmic energy decrement of the mixture. A correction can, therefore, be applied to F(E), but it is not yet included in the group set presented here.

Correctly the denominators in (1) should contain in NR approximation the total macroscopic cross-section of the mixture under consideration. For practical purposes it is convenient to replace the cross-section of the rest materials by an appropriate average in group g. Usually one takes the infinite dilute total group cross-sections in group g for this average, but it is very unrealistic to take the average total cross-section of $^{238}U$ with a resonance level spacing of 18 eV as a background for the shielding of $^{235}U$ or $^{239}Pu$ resonances with level spacings of roughly one order of magnitude less. Therefore, we defined ${}^{k}\sigma^{g}_{o} = \frac{1}{N_k} \sum_{m \neq k} N_m {}^{m}\sigma^{g}_{t}$, with ${}^{238}\sigma^{g}_{t}$ replaced by the potential scattering cross-section.

The effective group cross-section is splitted into two parts:

$$(2) \qquad {}^{k}\sigma^{g}_{z} = {}^{k}\sigma^{g}_{z,\infty} \cdot {}^{k}f^{g}_{z}(T,\sigma^{g}_{o})$$

${}^{k}\sigma^{g}_{z,\infty}$ is the group constant for infinite dilution for T=0 and T is the average temperature of the fuel. Both factors are tabulated on the Karlsruhe GROUCO file. This splitting procedure is very useful in the statistical resonance region, because there ${}^{k}\sigma^{g}_{z,\infty}$ is then calculated by integration over pointwise tabulated microscopic cross-sections, while the self-shielding factor is determined by statistical resonance parameters. By this procedure the influence of uncertainties in statistical parameters is reduced.

The evaluation of the self-shielding factors is based on the single level Breit-Wigner formula. Interference of potential and resonance scattering and resonance overlap is taken into account. The detailed description of the calculational technique will be given in the full documentation of the SNEAK-set.

For the description of elastic moderation the $\sigma_o$-concept has been abandoned, the dependence on the mixture is taken into account in NR approximation exactly in each reactor calculation. For high energy anisotropic scattering in the CMS system the known experimental angular distributions are directly inserted and integrated over the degradation interval. For the essential energy region of the important resonances the provided experimental data are sufficient, they are currently completed. The automatic calculation of the macroscopic elastic removal group cross-section in every diffusion run necessitated a reorganisation of the KEDAK-file, which resulted in a new ERDAK-file which is used in these calculations.

The transport cross-section is defined by

$$\sigma^g_{tr} = \sigma^g_t - \sum_{j \leq g} \sigma^{j \to g} \cdot \mu^{j \to g} \qquad (3)$$

where $\sigma^{j \to g}$ is the scattering matrix (calculated with the appropriate weighting F(E)) and $\mu^{j \to g}$ are the elements of the matrix for the average scattering cosine. Equ. (3) is based on the assumption that the neutron current is only weakly dependent on energy at least whithin the most important groups directly neighboured to group g. In the SNEAK-set up to now only hydrogen is treated by equ. (3), because for isotopes with higher atomic weight than 10, the second term on the right hand side of equation (3) can be approximated by $\sigma^g_e \cdot \mu^g_e$ .

The inelastic scattering matrix is calculated taking the same transferfunction as in ABN but normalizing the matrix elements to the reevaluated total inelastic cross-section. The (n,2n) processes are included in the inelastic matrix.

The various ; codes for calculating the group constants are combined in the code system MIGROS. The organisation is given in Fig. 1. Two different methods can be used in calculating the elastic moderation: method A is based on the $\sigma_o$ concept, method B calculates directly the shielded macroscopic elastic removal from the ERDAK-file. The code system is fully automized which is important especially for the determination of shielding factors in the different energy regions of resolved, statistical and strongly overlapping resonances.

## 2.2. Comparison of Group Constants

The SNEAK-set contains new group constants, based on a reevaluation by J.J. Schmidt, for the following elements or isotopes:

H, C, O, Na, Al, Cr, Fe, Ni, $^{235}U$, $^{238}U$, $^{239}Pu$.

The cross-sections for other isotopes are up to now identical with those given in the ABN-set. New group constants will be provided also for fission products [6] and the higher Plutonium isotopes [7], but these data had not yet been included on the KEDAK and GROUCO files during the analysis which is discussed in this paper.

As mentioned above, all new effective group cross-sections are weighted with the collission density F(E) which had been obtained by smoothing the core averaged F(E) of a diffusion calculation with KFK 26-10 for SNEAK 3A-2 with the hydrogen density of 0.07 g/cm$^3$. Only the main differences in the group constants of the SNEAK-set compared to KFK 26-10 and ABN-set are shown here.

Fig. 2 shows the fission and capture group cross-sections for $^{235}U$. SNEAK data for capture between 10 keV and 500 keV are smaller by 10-20 % than the KFK-data, the fission values, based on the measurements of White show the same behaviour, the deviations are somewhat smaller, however. The low $\sigma_c$-values result from lower $\alpha$-data in this energy range.

Capture and fission group cross-sections for $^{239}Pu$ are given in Fig. 3. Between 10 and 100 keV the fission data are taken from White measurements (in ref. [4] these values had not yet been recommended), and the low capture values result also from smaller $\alpha$-data. The new data are smaller by 10 - 20 % compared to the previous KFK-data.

The capture cross-sections for Cr, Fe, and Ni practically are the same as in the KFK 26-10 set. It should be noted again the large differences in the region 10 keV - 100 keV, where the values used in Karlsruhe for $\sigma_c$(Fe) (Moxon measurements) are about a factor 2-3 larger than the Russian constants, for $\sigma_c$(Ni) especially between 10-20 keV there is a factor of 4.

The Al-capture group constants in the SNEAK-set are larger than the ABN values in the essential energy region between 10 keV 500 keV by 20 % up to a factor of 2. Also in the low energy region we have larger capture values. The microscopic data for Al are taken from AEEW - M445 with only slight modifications.

In Fig. 4 the group constants for neutron capture in $^{238}U$ are shown. The "SNEAK"-values differ in the energy region from 20 eV up to 1 MeV by roughly 10-20% from the Russian data, compared to the first KFK-data the new group constants are larger by about 10-15% between 1 keV and 20 keV, smaller by about 20% in the region 0.2 keV-1 keV and 10 eV - 50 eV. The recommended capture data between 1-10 keV are calculated values from statistical theory and are just in between the measured data by R.L. Macklin et.al. (1964) and M.C. Moxon et.al. (1964). Very recently Pönitz and Menlove in Karlsruhe have measured the $^{238}U$ capture cross-section in the region between 10 keV and 500 keV [8]. These data are denoted in Fig. 4 by PM and are smaller than the SNEAK-data by about 7-15%

In Fig. 5 the self-shielding factors for $\sigma_o$=100 barn and T=900°K calculated with the recommended resonance parameters are compared with the equivalent ABN-data. Between 10 eV and 1 keV the SNEAK-values are larger by 10-30%.

In order to see the influence of the different methods in calculating the macroscopic elastic removal cross-section, the results for the SNEAK-set are plotted in Fig. 6. Method A is based on the $\sigma_o$ concept, method B calculates the macroscopic group constant directly from microscopic data in each reactor calculation. Because the escape probability for a neutron scattered out of a group varies strongly within the degradation interval, and this interval for all isotopes except the very light ones is small against the group width and comparable to resonance widths of e.g. iron or oxygen, the removal cross-section of any isotope except the very light ones is strongly influenced by the resonance structure of the macroscopic total cross-section of the mixture. For the SNEAK-assembly in two groups this influence is remarkable. In the group from 400 keV to 800 keV the oxygen resonance at 442 keV reduces the removal cross-section of all isotopes except hydrogen in method B, because the escape probability, weighted by the ascending wing of the total cross-section of oxygen in method B, is smaller than in method A, where only an average total cross-section is used. In the group from 21.5 keV to 46.5 keV the descending wing of the asymmetric resonance dip of iron at 25 keV causes a larger escape probability for all isotopes except hydrogen by method B than by method A. Therefore, the removal cross-section is enlarged by method B. These effects can plainly be seen in the corresponding neutron spectra, shown in fig. 11. The differences to the Russian removal data are quite large in the resonance region of structural materials, because besides of the different

weighting spectrum the infinite dilute value of the elastic scattering group constants as well as the corresponding shielding factor which enter the elastic removal cross-section are calculated for the total energy group and not for the degradation interval only.

Formula (3) yields a higher transport cross-section down to the keV-region for hydrogen, and as a consequence the leakage of fast neutrons out of the system will be reduced. The previously used $\sigma^H_{tr}$ data are calculated by $\sigma^H_{tr} = \sigma^H_s \cdot (1-\bar{\mu}) + \sigma^H_a$ where the average cosine of scattering is given by 2/3. Fig. 7 shows the differences.

## 3. RESULTS

### 3.1 Results obtained during Preparation of KFK-SNEAK

The new constant set was prepared in a similar way as the first set KFK 26-10. As a basis we have taken the Russian ABN set and have replaced the group constants of the elements and isotopes mentioned above by new ones. After each replacement a fundamental mode diffusion calculation for the homogenized core using method A for elastic removal was performed to determine the influence of the new data on integral reactor quantities. The core composition is that of the assembly SNEAK 3A-2 with a hydrogen density similar to a larger steam cooled fast reactor. The atomic number densities of the core materials are (the factor $10^{24}$ has been omitted): $N(Al)=1.289 \cdot 10^{-2}$, $N(C)=8.62 \cdot 10^{-4}$, $N(Cr)=1.27 \cdot 10^{-2}$, $N(H)=1.64 \cdot 10^{-3}$, $N(Ni)=1.86 \cdot 10^{-3}$, $N(O)=1.446 \cdot 10^{-2}$, $N(^{235}U)=2.034 \cdot 10^{-3}$, $N(^{238}U)=8.108 \cdot 10^{-3}$.

The fundamental mode calculations were performed in two different ways: (1) achieving criticality by iteration of the buckling, (2) taking the critical buckling from a calculation with the ABN-set and looking for the difference in criticality produced by the special replacement considered. The new group cross-sections for the various isotopes were replaced in the following sequence: (1) $^{238}U$, (2) $^{16}O$, (3) Fe, (4) Cr, (5) $^{12}C$, (6) Ni, (7) Al, (8) H, (9) $^{235}U+^{239}Pu$, (10) $\sigma_p$ $(^{238}U)+\sigma^H_{tr}$, (11) Na.

In the figures 8-10 this sequence is numbered from 1 to 10, 1 corresponds to the replacement of $^{238}U$, 2 to the additional replacement of oxygen, replacement 10 introduces the potential scattering cross-section of $^{238}U$ for $\sigma_o$ determination and the $\sigma^H_{tr}$ according to equ. (3). With replacement 10 all ma-

terials,which build up the core composition of the SNEAK assembly, are inserted in the set. Na has been replaced afterwards. On a separate tape we replaced the $^{238}U$ capture data recommended by Schmidt by the recent data of Pönitz and Menlove (PM-data), all other materials are the same as in the SNEAK set.

Fig. 8 shows the behaviour of $k_{eff}$ and $k_\infty$ during the preparation procedure related to the corresponding values obtained with the ABN set, Fig. 9 the total capture rate, $^{238}U$-capture rate and the $^{235}U$-fission rate, in Fig. 10 the integral quantities conversion ratio (CR), Doppler coefficient (DC) and neutron generation time ($\ell$) are given. In all the figures also the corresponding results obtained with the KFK 26-10 set and with the PM-capture data for $^{238}U$ are included. The results of Fig. 8 are calculated with that buckling which produces $k_{eff}=1$ for the ABN set, all data in Fig. 9 and Fig. 10 are taken from the corresponding critical system.

With the replacement of $^{238}U$ data into the ABN set there result less neutrons in the high energy region (larger inelastic scattering by about 15-10% in the region between 0.8 and 2.5 MeV) and more neutrons below 100 keV, mainly due to the changed capture data which are lower by about 15% between 50 keV and 400 keV compared to the ABN data. This spectral shift causes a small decrease in the $^{238}U$ fission rate, an increase in $^{238}U$ capture by 1%, (the average effective capture cross-section increases by about 2%), and as a consequence $k_{eff}$ becomes smaller. The larger (1%) DC and CR are also due mainly to the spectral shift mentioned.

The oxygen replacement (2) results in a further softened spectrum, mainly because of the different weighting spectrum. (F(E)=1/E in ABN), giving higher capture rates, CR, DC and $\ell$. $k_\infty$ is reduced because of larger absorption, but the leakage is even more reduced because at high energies more neutrons are slowed down thus giving a smaller leakage component in the important high energy region. For large reactors the $k_\infty$ effect dominates the leakage effect.

The replacement of iron (3) merely results in an increase of the total capture rate giving less reactivity. This is caused by the higher capture cross-section (factor 2) in the new set.

As the volume percentage of Cr, C, Ni is small in the SNEAK core, the effects of the replacements 4-6 are small.

Because of the better down scattering at high energies (weighting function) the Al replacement (7) gives less neutrons above 200 keV, more neutrons between 200 keV to 20 keV, and again less neutrons below 10 keV. Thus, the leakage is reduced, showing a larger $k_{eff}$ because $k_\infty$ is unchanged. The smaller number of neutrons below 10 keV is responsible for the remarkable decrease in DC. Hydrogen (case 8) scatters down more neutrons above 200 keV and less neutrons below because of the different weighting spectrum. This gives higher total capture rates and especially a remarkable increase in DC and $\ell$. The decrease in $k_\infty$ is just compensated by the simultaneous decrease of the leakage rate. One should note, however, that already in the ABN set we used equ. (3) for calculating the transport cross-section, and in replacement 8 for organisatoric reasons we had to take the usual $\sigma_{tr}$ definition. Thus, in this case the hydrogen is somewhat more transparent than in the other calculations 1-7. The correction for $\sigma_{tr}$(H) is performed in replacement 10. The ninth replacement of $^{235}U$ gives by far the largest effects. The spectrum is softer because of a larger reduction of capture at lower than at higher energies. Thus, especially the capture in $^{238}U$ becomes considerably larger by 10%, the fission and absorption become smaller on account of the lower cross-sections in spite of the softer spectrum. In consequence $k_\infty$ becomes smaller (1%),and as the leakage rate is also greater $k_{eff}$ changes by about 1.7%. The larger capture in $^{238}U$ (spectrum effect) and the lower absorption in $^{235}U$ (effect of cross-sections) produce a 10% higher CR than in case 8. DC and $\ell$ are enlarged also roughly by 10% (spectrum).

Case 10 contains the replacement of the hydrogen transport cross-section according to equ. (3) (see also Fig. 7). Together with the new $\sigma_{tr}^{H}$ the potential scattering cross-section of $^{238}U$ $\sigma_p$=10.6 b has been introduced for the calculation of $\sigma_o$ due to the reasons mentioned in chapter 2.1. The leakage is somewhat decreased and overcompensates the decrease in $k_\infty$ on account of the slightly softer spectrum.

Case 10 now is identical with the KFK-SNEAK group set. (The sodium replacement has been done later, because SNEAK 3A does not contain Na.) With this set calculations have been performed for the core composition SNEAK 3A-1. The results of these calculations are compared with experimental results in the paper of D. Stegemann et.al. [5]. Before we will draw the essential con-

clusions, we will discuss the effects of another cross-section replacement based on the recent measurements of the capture cross-section by Pönitz and Menlove (PM data). We obtained these data at a time, when the calculations with the SNEAK set were almost completed and for consistency they are not included in the theoretical results of ref. [5]. For the reference core composition discussed in this chapter (SNEAK assembly 3A-2) the lowered $^{238}U$ capture results in an increase of $k_{eff}$ by 0.9%, the CR is lowered by 0.5%.

In Fig. 11 and Fig. 12 the neutron spectra and adjoint spectra of the SNEAK 3A-2-core are shown for different sets and methods related to the values of the ABN set: in Fig. 11 the spectra calculated by method A and method B are given (for discussion see chapter 3.1). The sharp dip in the sodium resonance group 13 in the KFK 26-10 arises from the elastic removal cross-section (method A) of $O^{16}$, which follows the Na resonance shape because of the weighting spectrum of a sodium cooled reactor used in KFK 26-10. The changes in neutron importance can easily be understood by considering the changes in the $^{238}U$ capture and $^{235}U$ fission and capture group cross-sections given in Fig. 2 and Fig. 4.

In Table I we listed the changes in the loss of coolant reactivity $\Delta k_L$ and the reduced steam density coefficient of reactivity $\frac{dk/dk}{d\rho/\rho}$, both related to ABN-values. The results can plainly be understood by following the discussion given before. Again the largest differences are obtained in the $^{235}U$ replacement in case 9. One should note the 20% decrease in $\Delta k_L$ and 11% increase in the reduced steam density coefficient compared to ABN. The KFK 26-10 set gives results in between the ABN and SNEAK set, because a great part of microscopic data are similar to those incorporated in the SNEAK-set. As we performed fundamental mode calculations using the critical ABN buckling, only the trends should be given precisely; clearly the absolute values must be obtained in 1- and 2-dimensional calculations.

## 3.2. Main Results for the SNEAK 3A-1 Assembly Obtained with the KFK-SNEAK Set

The detailed comparison of experimental and theoretical results obtained with the KFK-SNEAK set (method B) for the assembly 3A-1 is given in ref. 5. Here we will quote the main results to get an impression of the quality of data and methods used.

(a) Criticality

| | | |
|---|---|---|
| Homogeneous two dimensional diffusion theory, method B: | $k_{eff}^{hom}$ | = 0.9895 |
| $S_4$-correction: | $\Delta k(S_4)$ | = +0.0027 |
| Heterogeneity correction: (calculated) | $\Delta k(het)$ | = +0.0025 |
| So we have | $k_{eff}^{het}$(SNEAK) | = 0.995 |
| For comparison: | $k_{eff}^{hom}$(ABN) | = 1.019 |
| | $k_{eff}^{hom}$(KFK 26-10) | = 1.018 |

Accuracy of half a percent in $k_{eff}$ is the target of reactor calculations and this is achieved with the group set KFK-SNEAK. It should be noted again that no adjustments to measured reactor quantities have been made. Both KFK-26-10 and ABN give higher $k_{eff}$ values by about 3%!

(b) Spectrum and Spectral Indices

In Fig. 13 the spectra calculated with the SNEAK set (method A and method B) and with the KFK 25-10 set are compared with experimental results. Again we have a satisfying agreement between theory and experiment for method B and the SNEAK set. The less accurate method A gives 20% deviations in the most important groups for elastic scattering (oxygen and iron resonances). Inserting the PM data into the SNEAK set, the spectrum is practically unchanged. The result can be improved by one iteration step for the collission density. From the spectrum, calculated by SNEAK-method B, a new collission density can be obtained, which is used for calculation of new removal cross-section in another SNEAK-method B calculation. This is not yet done in this paper. The effects should not be large.

In Table II the most important fission and capture to fission ratios for the centre of SNEAK 3A-1 are compared to experiment. There is very good agreement in the $^{238}U$ capture to $^{235}U$ fission ratio, the other ratios do not fit as well to the experimental data. A check has been made in using the measured spectrum in the calculation of $\sigma_f(^{238}U)/\sigma_f(^{235}U)$, giving no improvement. This effect is not yet understood and needs further investigation, especially with respect to the experimental technique used.

In Table II also the corresponding ratios are given using the low $^{238}U$ capture data of Pönitz and Menlove. The drastic reduction in $\sigma_c(^{238}U)/\sigma_f(^{235}U)$ is just within the experimental error line. With respect to criticality we obtain with the PM-data $k_{eff}^{het}(PM) = 1.008$, applying the same corrections for $S_4$ and heterogeneity given above. There is a strong indication that because of normalization corrections the fission and capture cross-sections of $^{235}U$ should be even smaller than the low White data included in the SNEAK-set [10]. This would result in better agreement of the PM-data with experiment. The influence of these renormalization effects on the important integral nuclear quantities is being investigated.

(c) Heterogeneity Corrections

The SNEAK-set gives far better agreement with the experimental results than both KFK 26-10 and ABN set [5], [9]. The theory results in about 10% higher $\Delta k^{het}$ than the measured results in the bunching experiments, while ABN-data are too small by a factor of two in $\Delta k^{het}$. Also the detailed cell fine structure gives much better results if the SNEAK-set is used instead of ABN or KFK 26-10.

(d) Void Calculations

The sequence of void measurements in the central zone of SNEAK 3A-1 is fairly well represented by calculations with the SNEAK-set [5]. Including heterogeneity corrections, there are deviations from experiment by about 5%. Results obtained with the ABN-set are 30-40% too low (see also ref. [9].)

(e) Breeding Ratio

Having in mind the theoretical and experimental results for the $^{238}U$ capture to $^{235}U$ fission ratio (Table II), also the breeding ratio of the SNEAK 3A-1 is in much better agreement with experiment than results obtained with KFK 26-10 or ABN, see also ref. [5].

3.3. Results for the ZPRIII/48 Critical Assembly

To check especially the Plutonium data incorporated in the SNEAK-set, we performed a calculation for the ZPRIII/48 assembly and compared the results with those formerly obtained with the KFK 26-10 set [11]. This first calcu-

lation for the homogenized core was done with that core radius, for which the KFK 26-10 set produces $k_{eff}^{hom} = 1.0$. With the SNEAK-set we obtained then $k_{eff}^{hom}(SNEAK) = 0.963$. The following corrections have to be made:

| | |
|---|---|
| $S_4$-correction | 0.003 |
| Heterogeneity correction (as given in the ANL intercomparison) | 0.014 |
| KFK 26-10 to experiment (as given in the ANL intercomparison) | 0.011 |

Thus, on the basis of the ANL intercomparison we obtain with the SNEAK-set

$$k_{eff}^{het}(SNEAK) = 0.991$$

In Table III some spectral indices are shown. Again as in the case of SNEAK 3A-1 the agreement is not too good. A more precise calculation for the real geometry of ZPRIII/48 with redetermined heterogeneity corrections is under way.

## 3.4. Results for Large Fast Power Breeders

For completeness some calculations have been done with the SNEAK-set for a steam cooled large power reactor, the Karlsruhe D1 design [12]. For the Karlsruhe prototype Na2 with sodium as a coolant a separate group set was established with the appropriate core weighting spectrum and an additional blanket weighting spectrum. This set is named KFK-NAP [13]. The most important feature is an expected reduction in $k_{eff}$ by about 2-3% for both types compared to results obtained with KFK 26-10. This means a difference in $k_{eff}$ by about 6% compared to ABN calculations. For the steam cooled reactor both coolant loss reactivity change $\Delta k_L$ and the absolute value of the steam density coefficient are increased remarkably, changing the stability characteristics of this reactor to the worse. These investigations are not yet completed.

## 4. CONCLUSION

The comparison of the theoretical results, obtained with the new group constant set KFK-SNEAK, with the measured results for the fast critical assembly SNEAK 3A-1 show a remarkable and encouraging step forward in the field of fast reactor calculation. Compared to the previous KFK 26-10 set the main

reasons for the better agreement of experiment and theory is caused by the low fission and capture data of $^{235}U$ included in the SNEAK-set and in an improved description of elastic moderation (method B). The remaining differences have to be analysed very carefully in order to get an idea of what has to be improved in microscopic cross-section evaluation and in the methods to establish macroscopic self-shielding group constants. On the theoretical side, for instance, we are dealing with the problem of space dependend resonance self-shielding (core-blanket interface), and in the near future we will have a code in consistent P1 approximation for 200 groups, so that the investigation of the space dependent fine structure of the spectrum will, hopefully, give further insight into the complex situation of fast reactor analysis.

Acknowledgement

We are very grateful to Dr. D. Stegemann to give us current access to experimental results.

REFERENCES

[1] I.I. Bondarenko et.al., Gruppenkonstanten schneller und intermediärer Neutronen für die Berechnung von Kernreaktoren, KFK-tr-144.

[2] J.J. Schmidt, Neutron Cross-sections for fast reactor materials, KFK 120, part I and part II.

[3] H. Küsters and M. Metzenroth, The influence of some important group constants on integral fast reactor quantities, ANL 7120 (1965) 432.

[4] J.J. Schmidt, Neutron cross-sections for fast reactor materials, KFK 120, part I.

[5] D. Stegemann et.al., Physics investigations of a 670 ℓ steam-cooled fast reactor system in SNEAK, assembly 3A-1, KFK 627, SM 101/11, this conference.

[6] R. Hakanson, 26-group cross-sections for the fission products in a fast reactor, internal KFK-report.

[7] S. Yiftah, J.J. Schmidt, M. Segev, M. Caner, Basic nuclear data for the higher Pu-isotopes, this conference.

[8] W. Pönitz and H.O. Menlove, Absolute radiative capture cross-sections for fast neutrons in $^{238}U$, Paper submitted for publication to Nuclear Science and Engineering.

[9] D. Wintzer, Heterogeneity calculations including space dependent resonance self-shielding, SM 101/13, this conference.

[10] K.H. Beckurts, private communication.

[11] K. Lieber and M. Metzenroth, Contribution to the intercomparison on ZPRIII/48, Conference on fast critical experiments and their analysis, Argonne, 1966.

[12] E. Kiefhaber, Reactivity coefficients of steam-cooled fast breeders, KFK 629, SM 101/15, this conference.

[13] H. Bachmann, M. Metzenroth, K.E. Schroeter, D. Woll, Der KFK-NAP Gruppenkonstantensatz, Erstellung und Ergebnisse, to be published.

Table I: Changes in Loss of Coolant Reactivity and Reduced Steam Density Coefficient during Preparation.

| | KFK 26-10 | 1 | 2 | 3 | 4 | 5 | 6 | 7 | 8 | 9 | SNEAK | PM |
|---|---|---|---|---|---|---|---|---|---|---|---|---|
| $\frac{\Delta k_L}{(\Delta k_L)_{ABN}}$ | 1.119 | 0.9325 | 0.8918 | 0.868 | 0.862 | 0.862 | 0.858 | 0.8198 | 0.8249 | 1.181 | 1.2008 | 1.180 |
| $\frac{dk/k}{d\rho/\rho}$ / $(\frac{dk/k}{d\rho/\rho})_{ABN}$ | 1.076 | 0.9478 | 0.914 | 0.911 | 0.907 | 0.907 | 0.904 | 0.883 | 0.892 | 1.096 | 1.107 | 1.077 |

Table II: Spectral indices in the center of SNEAK 3A-1

| | Experiment | SNEAK SET | KFK 26-10 | ABN | PM $\sigma_c$(U238) |
|---|---|---|---|---|---|
| $\frac{\sigma_f(U238)}{\sigma_f(U235)}$ | 0.0336±3% | 0.0301 | 0.0301 | 0.0316 | 0.0297 |
| $\frac{\sigma_c(U238)}{\sigma_f(U235)}$ | 0.142±0.008 | 0.143 | 0.129 | 0.127 | 0.136 |
| $\frac{\sigma_f(Pu239)}{\sigma_f(U235)}$ | 1.03 ±3% | 0.96 | 0.971 | 1.001 | 0.952 |

Table III: Spectral indices in the center of ZPRIII/48

| | Experiment | SNEAK SET | KFK 26-10 | ABN |
|---|---|---|---|---|
| $\frac{\sigma_f(U238)}{\sigma_f(U235)}$ | 0.0307 | 0.0301 | 0.031 | 0.0328 |
| $\frac{\sigma_c(U238)}{\sigma_f(U235)}$ | 1.38 | 1.45 | 1.31 | 1.30 |
| $\frac{\sigma_f(Pu239)}{\sigma_f(U235)}$ | 0.976 | 0.91 | 0.938 | 0.958 |

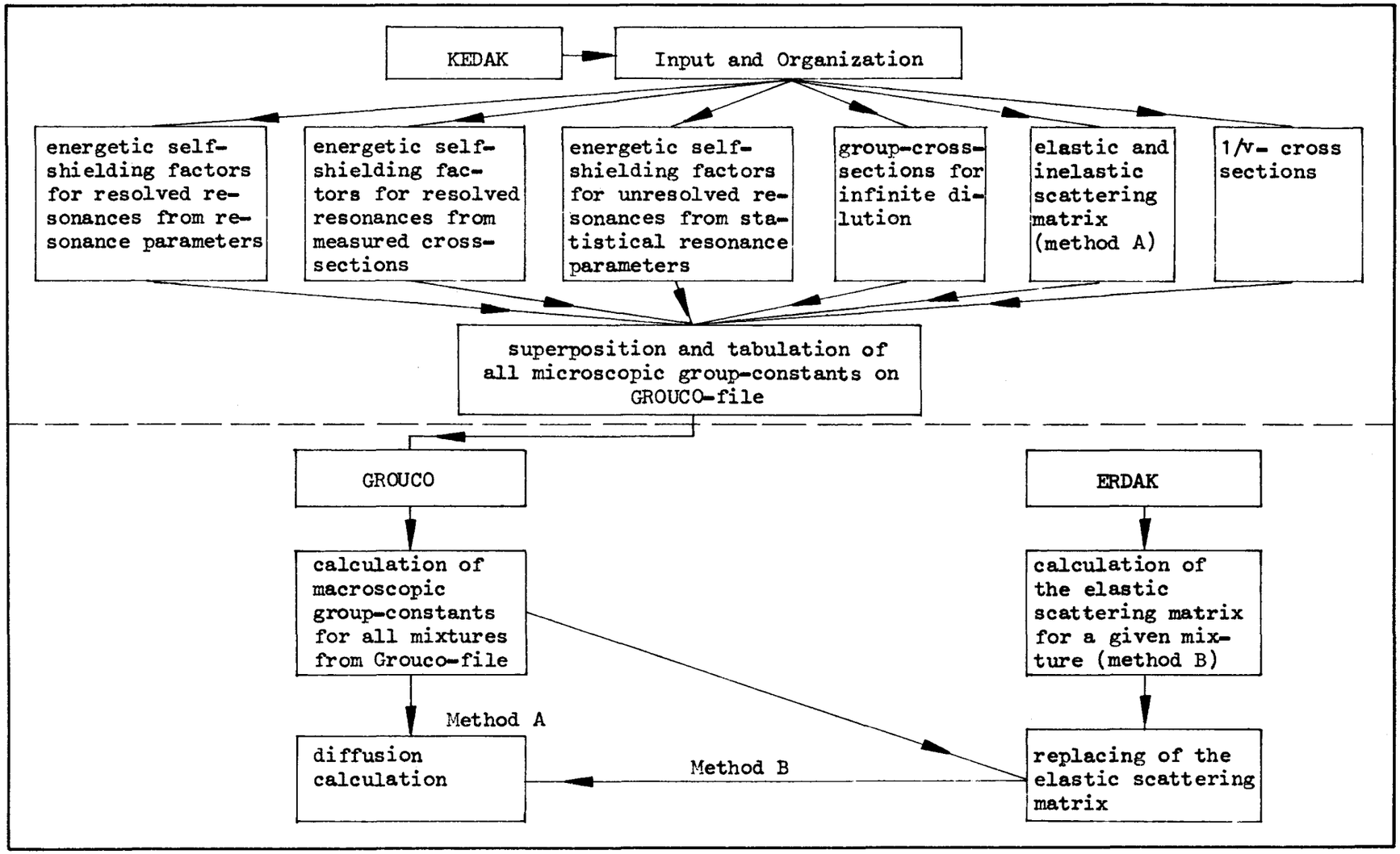


Fig. 1 The Code System MIGROS and the Preparation of Macroscopic Effective Group Constants.

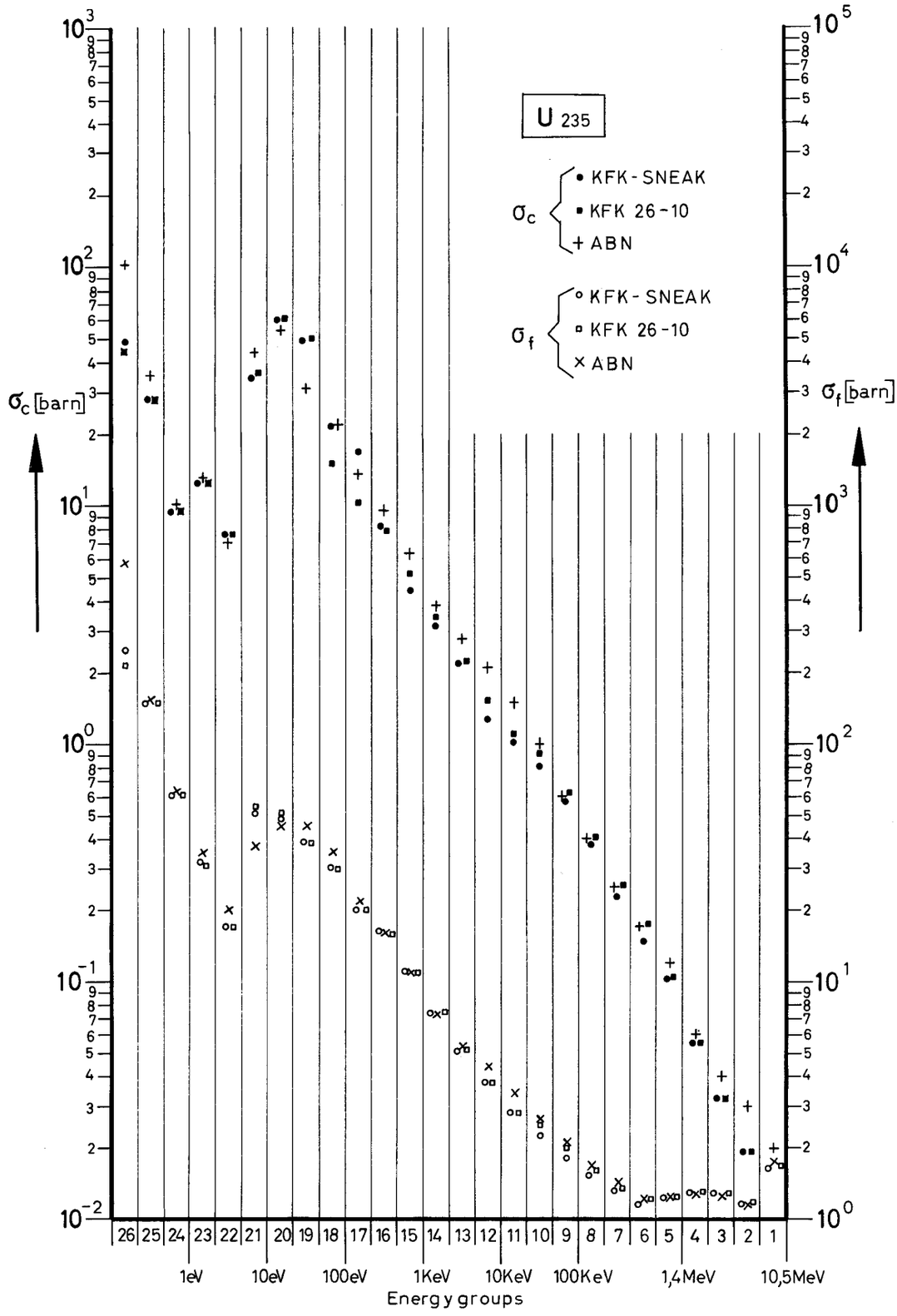


Fig.2 COMPARISON OF INFINITE DILUTE GROUP-CROSS-SECTIONS FOR CAPTURE AND FISSION OF U 235

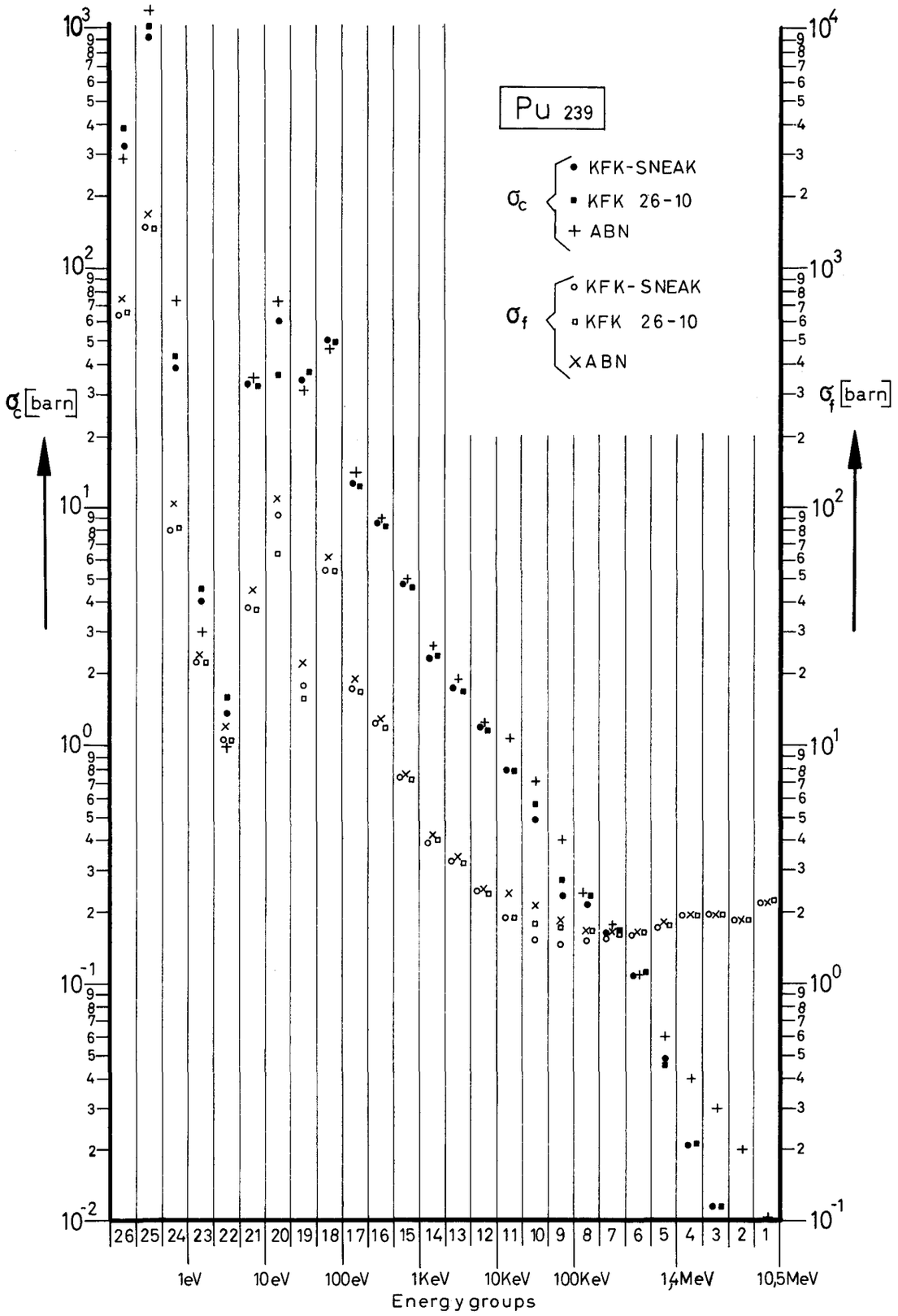


Fig. 3 COMPARISON OF INFINITE DILUTE GROUP-CROSS-SECTIONS FOR CAPTURE AND FISSION OF Pu 239

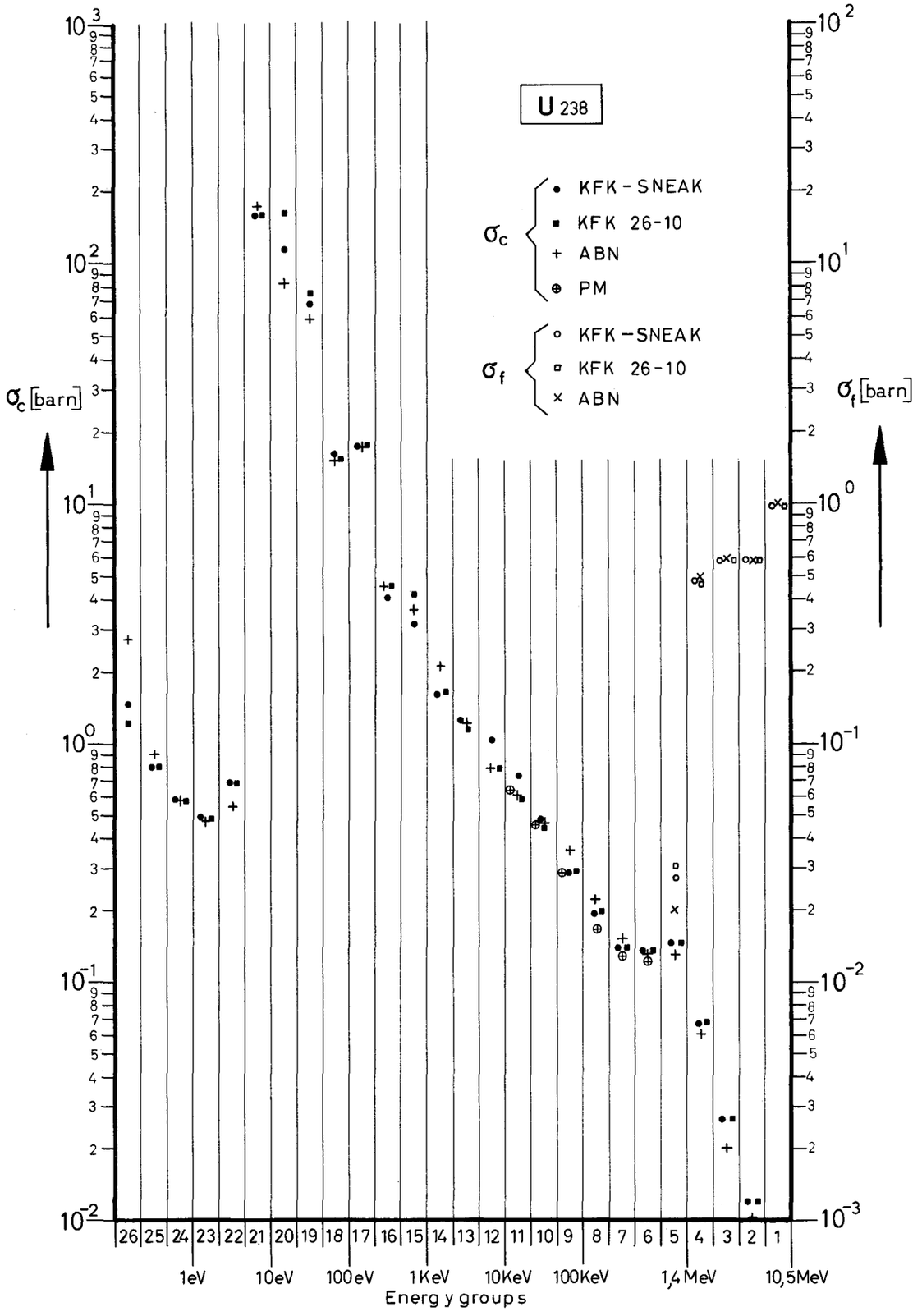


**Fig. 4** COMPARISON OF INFINITE DILUTE GROUP-CROSS-SECTIONS FOR CAPTURE AND FISSION OF U 238

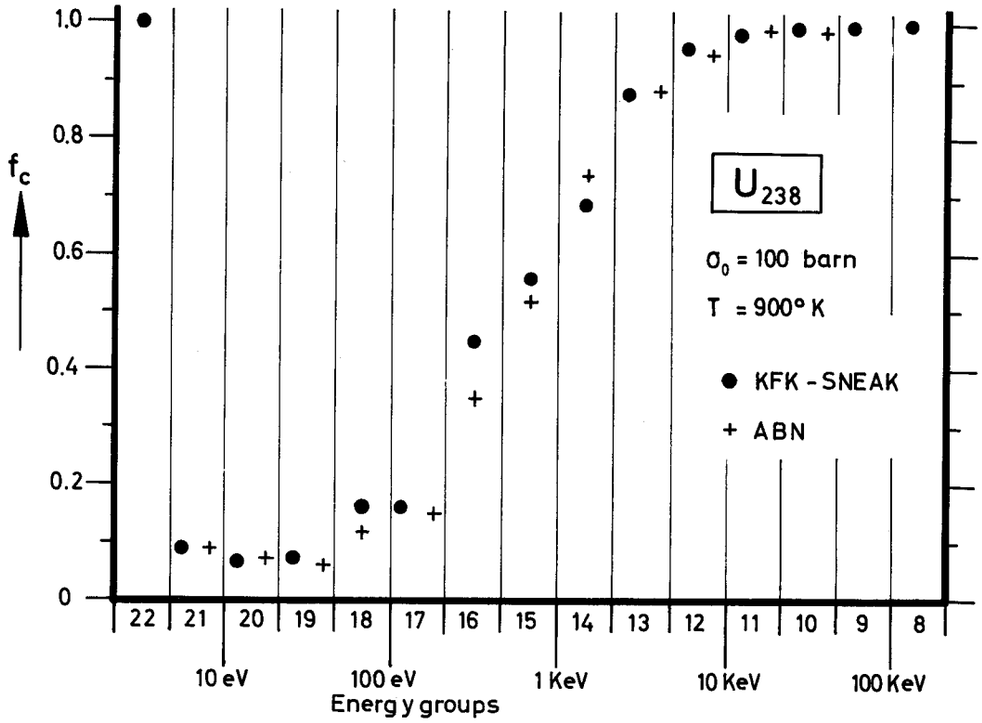


Fig. 5 COMPARISON OF ENERGETIC SELF SHIELDING FACTORS FOR CAPTURE ( $\sigma_0$ = 100 barn, T = 900°K ) OF U 238

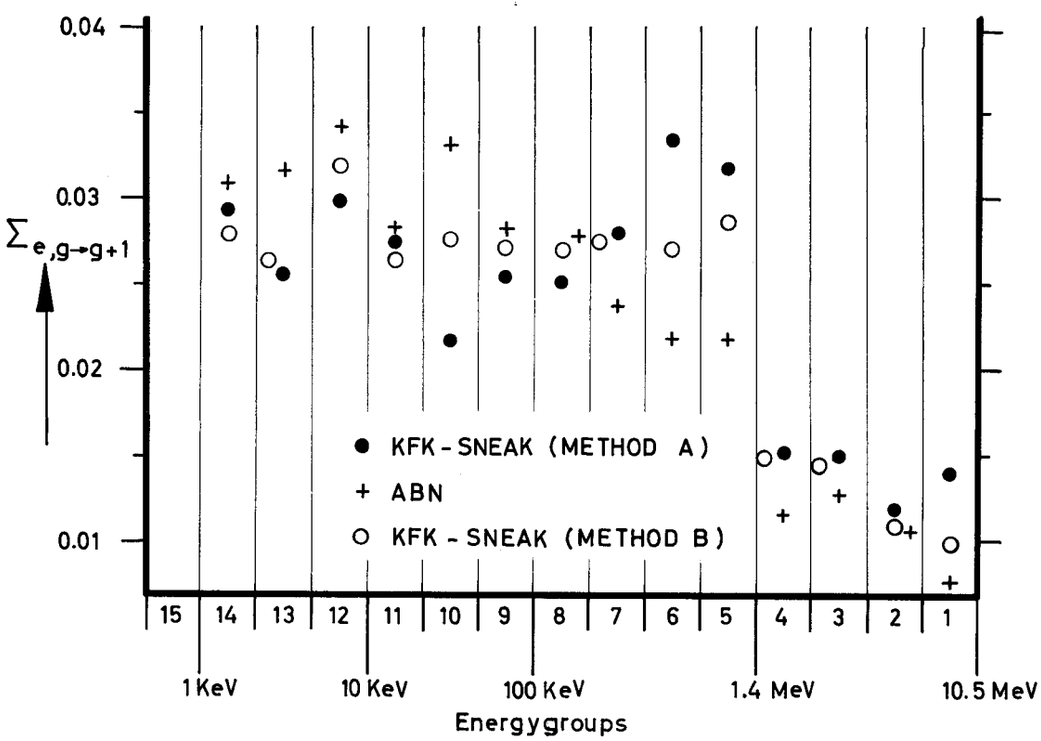


Fig. 6 COMPARISON OF DIFFERENT PROCEDURES IN CALCULATING MACROSCOPIC ELASTIC SCATTERING MATRIX (SEE TEXT)

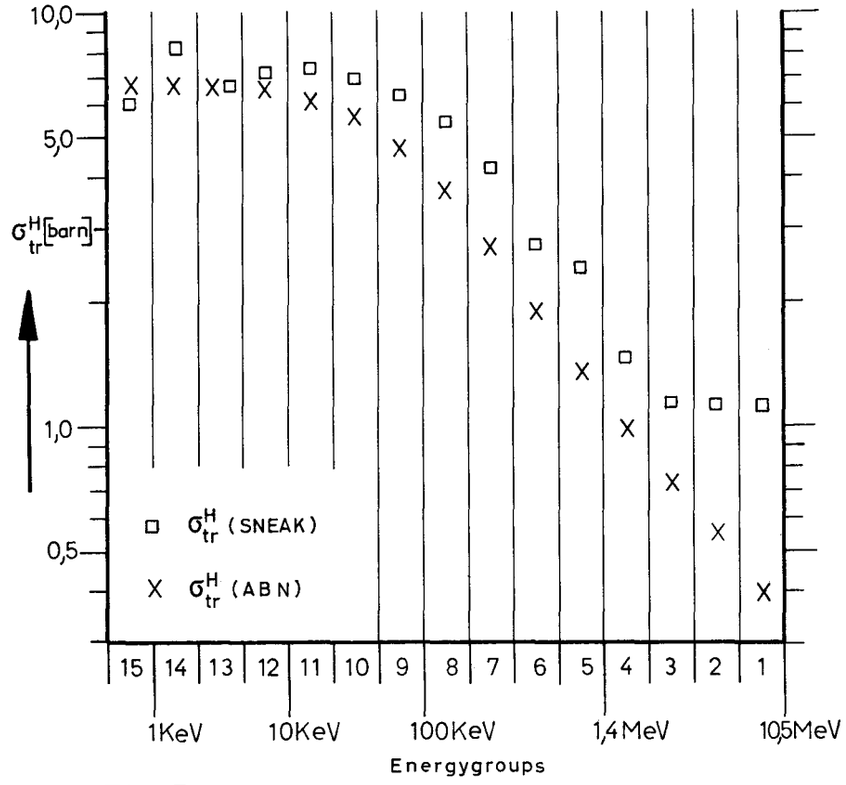


Fig. 7 COMPARISON OF THE TRANSPORT-CROSS-SECTION OF HYDROGEN

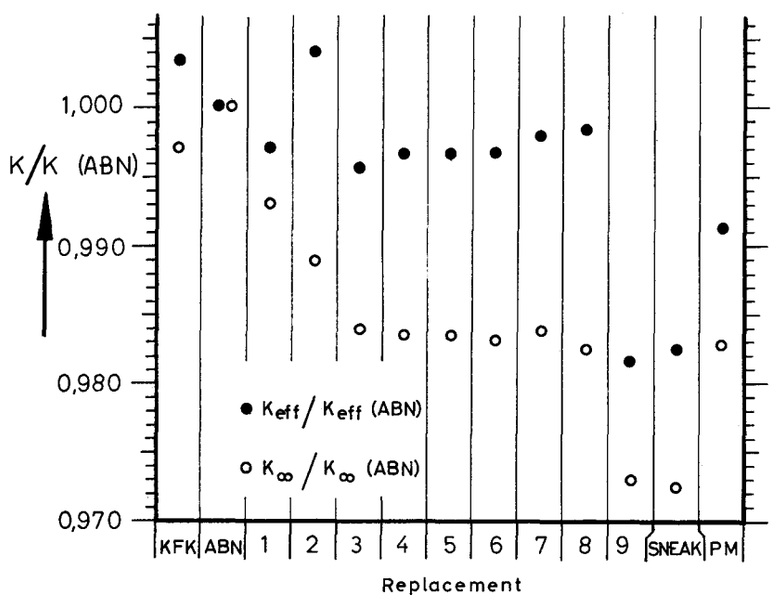


Fig. 8 CHANGES IN $K_{eff}$ AND $K_\infty$ DURING PREPARATION

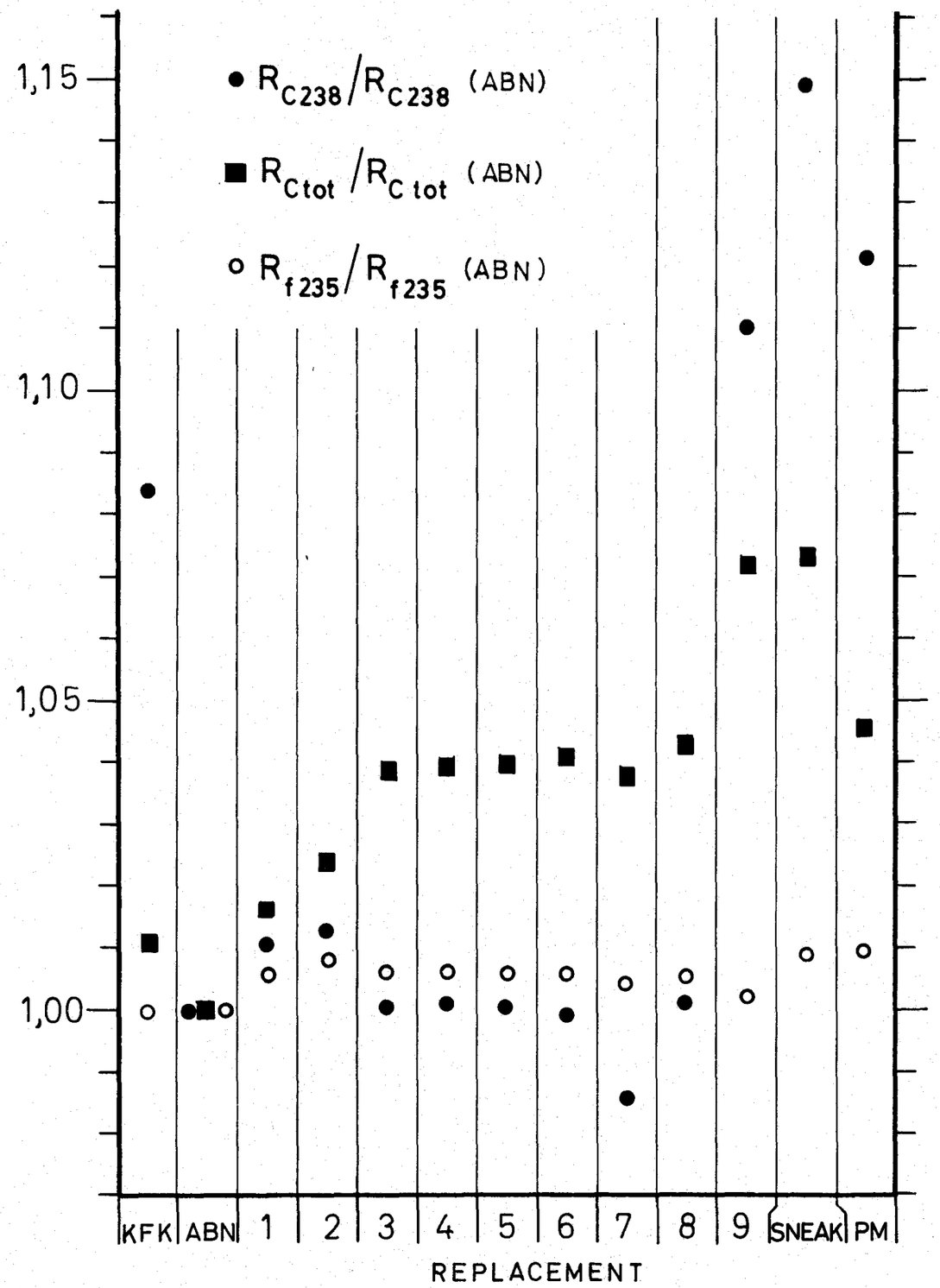


Fig.9 CHANGES IN REACTION RATES DURING PREPARATION

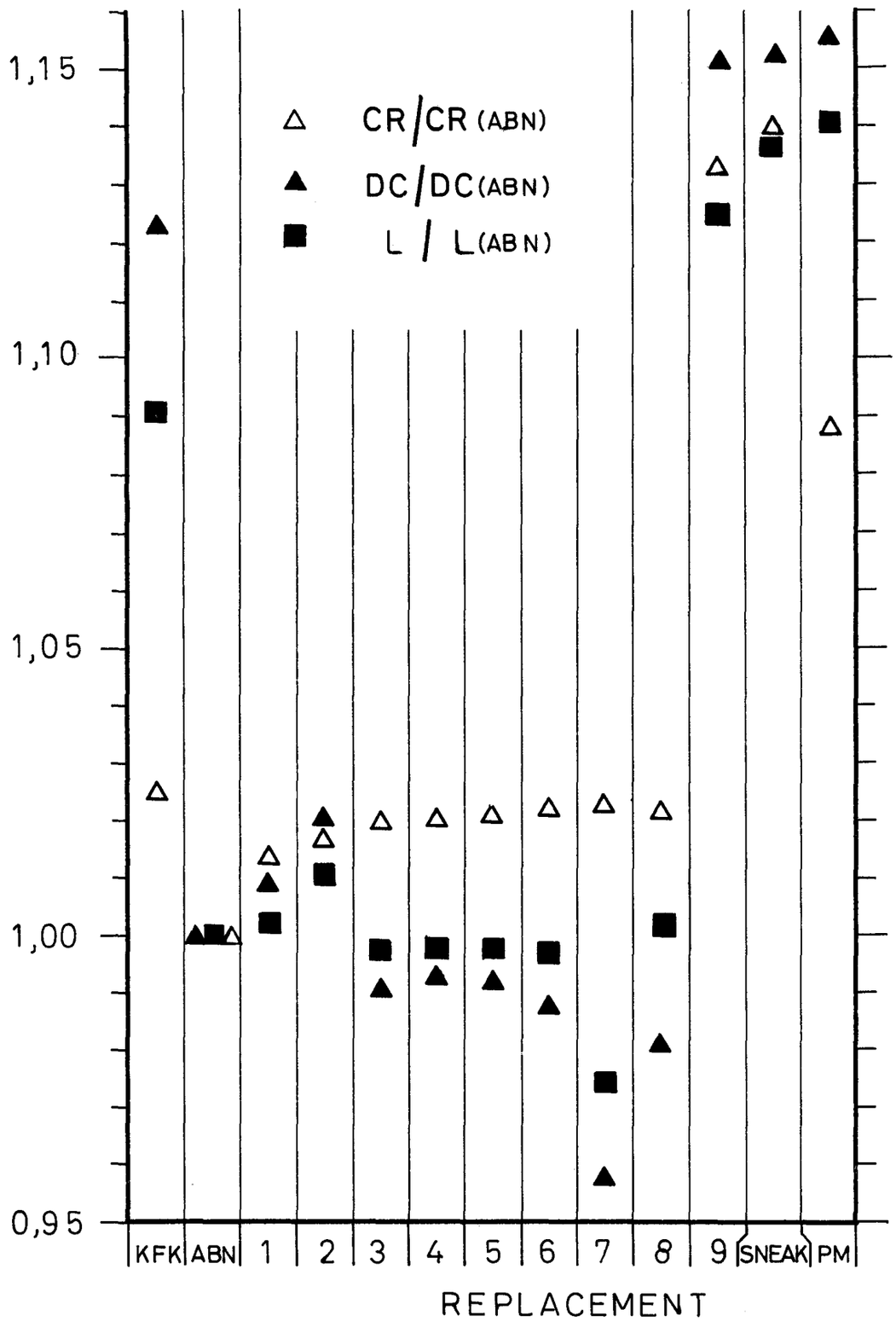


Fig.10 CHANGES IN INTEGRAL QUANTITIES DURING PREPARATION

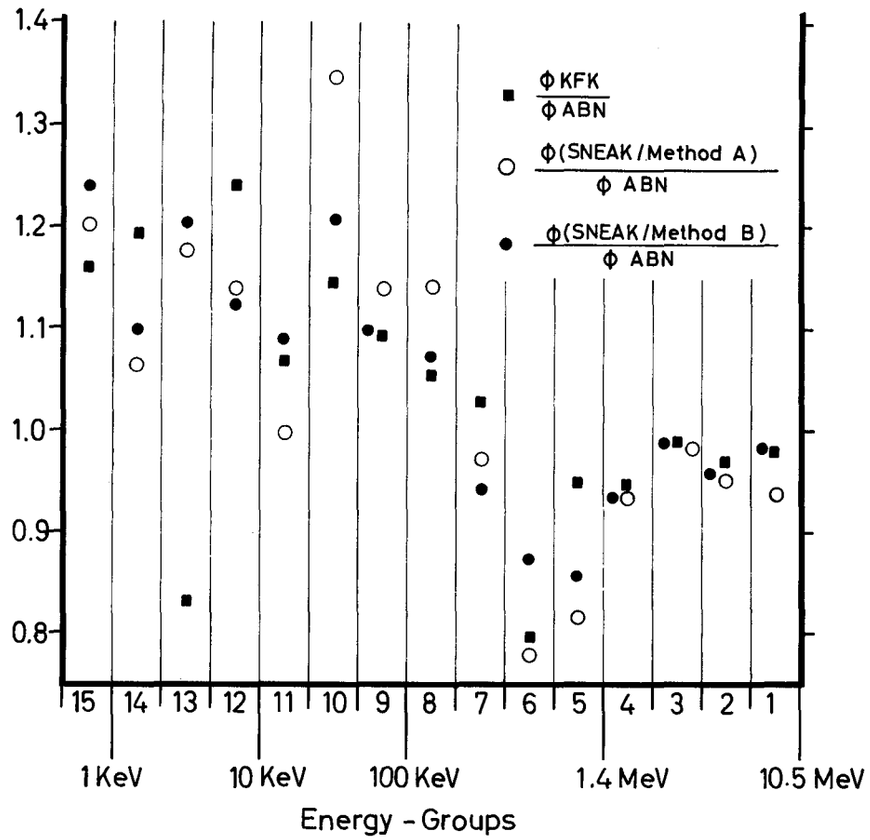


Fig. 11 COMPARISON OF NEUTRON SPECTRA

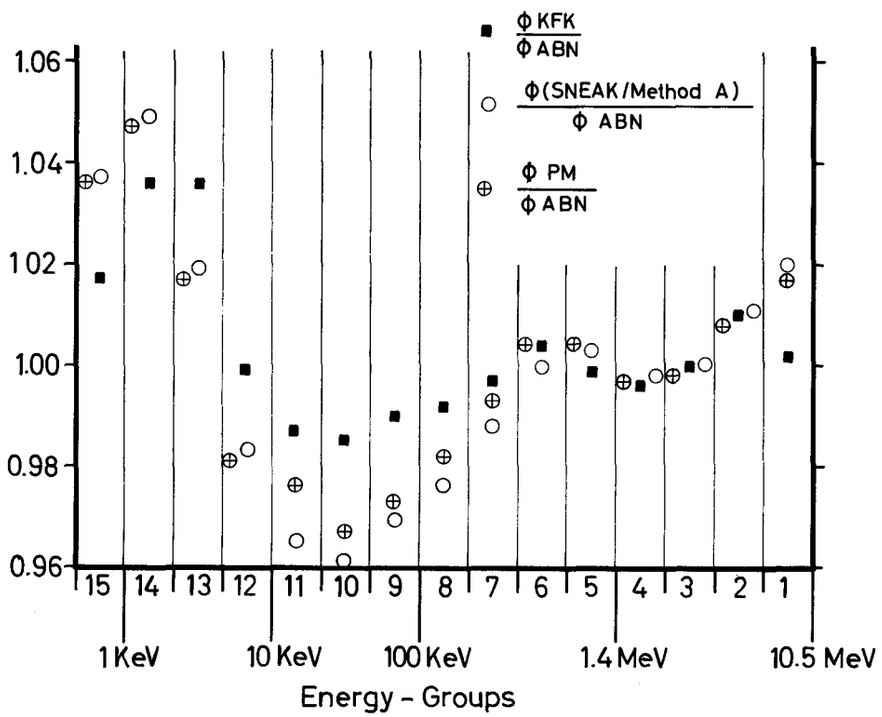


Fig. 12 COMPARISON OF THE ADJOINT FUNCTIONS

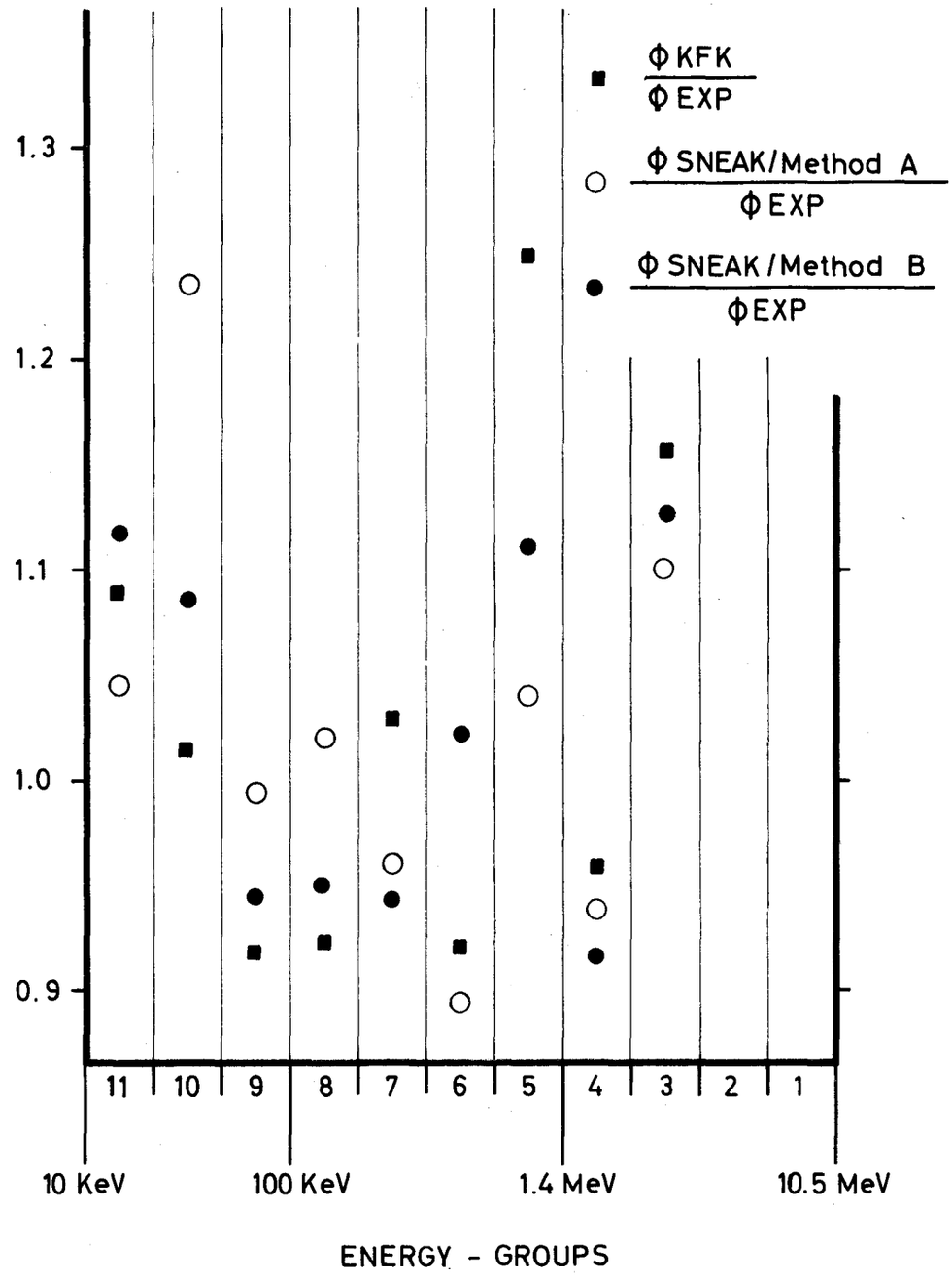


Fig. 13 COMPARISON OF THEORETICAL AND EXPERIMENTAL NEUTRON SPECTRA FOR ASSEMBLY SNEAK 3A-1